

Study of non-linear optical phase conjugation in Ca by resonant degenerate four-wave mixing via bound excited states

A. Bolovinos¹, S. Cohen³, A. Lyras¹, C. Skordoulis¹, T. Mikropoulos², S. Assimopoulos¹

¹ Atomic & Molecular Physics Laboratory, Dept. of Physics, Univ. of Ioannina, 45 110 Ioannina, Greece (Fax: +30-651/45631, E-mail: abolovin@cc.uoi.gr)

² Dept. of Primary Education, Univ. of Ioannina, 45 110 Ioannina, Greece

³ Institut de Physique Nucléaire, Université de Paris-Sud, 91 406 Orsay Cedex, Orsay, France

Received: 11 June 1996

Abstract. We have studied the optical phase conjugation (OPC) effect in Ca vapour by using the resonant degenerate four-wave mixing (DFWM) technique. The effect was studied through the first excited state of Ca, $4s4p\ ^1P_1$. The dependence of the reflectivity on the vapour density, the buffer gas pressure and the pump beams intensity was investigated. The influence of the strong linear absorption was taken into account in a theoretical model that led to a satisfactory interpretation of the experimental results. A maximum reflectivity of 46% was measured under optimized conditions. The effect was also studied through the high-lying bound states $4p^2\ ^3P_{0,1,2}$. The maximum measured reflectivity was as high as for the first excited state. The effect of the oscillator strength on the reflectivity was demonstrated experimentally and interpreted with the help of a simple theoretical model.

PACS: 42.65F; 42.65M; 32.80K

Optical Phase Conjugation (OPC) is a non-linear optical phenomenon, interesting for fundamental scientific reasons as well as for various applications [1]. Inducing OPC by the technique of Degenerate Four-Wave Mixing (DFWM) has a number of specific advantages over other techniques, the most notable of which is the automatic satisfaction of the phase-matching requirement [2] due to its particular geometry. The DFWM technique is based on the interaction of two counter-propagating pump beams, crossed by a probe beam, with a medium, whose non-linear response leads to the generation of a fourth beam. The generated beam has unique properties. Specifically, it has the same frequency as the input beams, it propagates exactly opposite to the probe one, and is its phase conjugate. Additional properties of the phase conjugated beam are its good directionality, the absence of an intensity threshold for its generation and the quadratic dependence of its intensity on the concentration of the non-linear medium. As a result, the DFWM technique has been considered as a powerful tool not only for spectroscopic [3] and analytical [4] investigations, but also for applications in optical signal and image processing [5].

It has been well established for some time now that metal vapours are suitable media for studying non-linear optical phenomena [6]. Up to now the studies of OPC by DFWM in metal vapours have been performed mostly in alkalis [2], considered to be ideal for the comparison between experimental results and the predictions of simple theoretical models [7]. Most of the existing theoretical models refer mainly to two- or three-level systems [7, 8] and steady state conditions, taking also into account the possible saturation of the atomic transitions [8], the effect of collisions with the buffer gas [9], the effect of absorption and depletion of the beams [10] and their propagation in the non-linear medium [11].

The alkaline earths are systems with two valence electrons and as a result their bound energy spectra are more complex than the corresponding ones in the alkalis. In the literature there exist few reports on the study of OPC by DFWM in alkaline earth atoms as, for example, in [12] where the effect was observed via the Ba resonance transition. The same technique has also been applied in Ca vapour [13], via the transition $4s^2\ ^1S_0 \rightarrow 4s4p\ ^1P_1$, aiming at the spectroscopic detection of the natural isotopes of Ca. In the alkaline earths Rydberg series of quasi-bound doubly excited states can be found above the first ionization threshold. These autoionizing states (AIS), as they are usually called, have been the subject of intense spectroscopic study in the last ten years [14]. Certain properties of great importance, e.g. their lifetimes, are rarely measured directly and can only be inferred by indirect and often not highly accurate measurements. The DFWM technique is suitable for the direct measurement of such spectroscopic properties with sufficient accuracy [1]. Other non-linear effects, e.g. harmonic generation [2] and laser-induced continuum structure [15], have been studied in the vicinity of AIS but OPC by resonant DFWM when an AIS is involved has not been reported so far. However, before one could proceed in such a demanding experiment more information on the non-linear response of the medium (in our case Ca) when highly excited states are involved should be obtained. This goal is served by the study of OPC via the manifold of the $4p^2\ ^3P_{0,1,2}$ states. This is one of the very few studies of OPC via highly excited bound atomic states [16]. Moreover, it should be noted that measuring lifetimes of bound Rydberg states is far from trivial and the

DFWM technique could be particularly useful in this respect as well. Also it can be helpful in studying the properties of atomic states whose fluorescence yield is particularly small, e.g. excited states of Ca that are forbidden to decay to the lower states by dipole transitions. A second goal is to check to what extent the OPC signal generated by resonant DFWM in an atomic species could be used reliably for non-intrusive monitoring of the conditions in a hostile environment (e.g. oven, flame, chemical reactor, etc.) in which the particular species is embedded. Most of the studies so far have dealt with molecular systems (e.g. OH) in flame environments [17]. Given the fact that the energy spectra and dynamics of molecular systems are quite different from the corresponding ones in atoms it is reasonable to expect that even if similar trends could be identified, the conditions under which they would appear could be quite different.

In the following we present results from the study of the OPC phenomenon by DFWM in Ca vapour via the $4s4p\ ^1P_1$ and $4p^2\ ^3P_{0,1,2}$ bound excited states. The study through the resonance transition ($4s^2\ ^1P_0 \rightarrow 4s4p\ ^1P_1$) is focused on the efficiency of the OPC phenomenon and its dependence on various externally controllable parameters such as the intensity of the pump beams, the pressure of the buffer gas and the Ca concentration in the vapour. A simple theoretical model taking into account the absorption of the beams from the medium is shown to satisfactorily reproduce most of the experimental results. Through these results it is possible to assess the usefulness of the OPC signal as a reliable diagnostic gauge of various quantities of interest, such as the Ca concentration in the vapour, and identify the range of parameters within which such an application is possible. The study through the manifold of the high-lying $4p^2\ ^3P_{0,1,2}$ is focused on the efficiency of the phenomenon and the effect of the atomic properties of each resonance (e.g. its excitation cross section and lifetime) on the strength and lineshape of the OPC signal. A simple model is adequate for the interpretation of the results, since beam absorption is not significant in this case. These results are an encouraging first step towards an observation of the OPC phenomenon by resonant DFWM through an AIS.

1 Experimental set-up

In Fig. 1 a simplified energy diagram of the Ca atom is drawn and the atomic transitions employed in our experiment are indicated. The experimental set-up was typical of the DFWM technique and is shown in Fig. 2. The light source was a dye laser system (the stilbene 420 dye (Exciton) was used) pumped by a N_2 laser, producing pulses of 5 ns duration and $\sim 0.4\text{ cm}^{-1}$ linewidth. For the resonance transition $4s^2\ ^1S_0 \rightarrow 4s4p\ ^1P_1$ the laser wavelength was scanned around the $\lambda_1 = 422.79\text{ nm}$, in order to obtain the OPC lineshape in the neighbourhood of the resonant state. The laser beam was splitted in three, generating two pump beams (one forward pump beam, FP, and one backward pump beam, BP) propagating in opposite directions and one probe beam (PB), propagating at an angle $\sim 1^\circ$ with respect to the FP. The three beams overlapped at the centre of the heat-pipe oven (HPO). As a result of their interaction with the Ca vapour a fourth beam, the phase conjugated (PC) one, was generated propagating in the opposite direction with respect to the PB. Special attention was given to the set-up geometry in order to achieve spatial and temporal overlap of

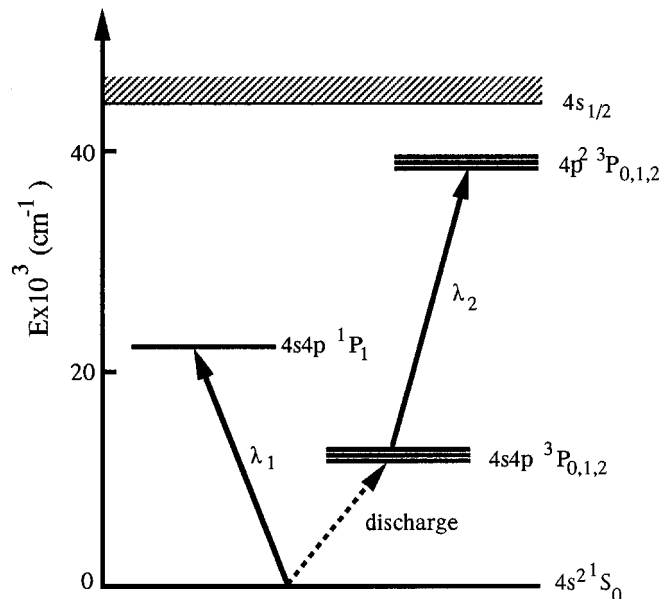


Fig. 1. Schematic energy level diagram for Ca. The transitions employed in the DFWM scheme are indicated by arrows. The discharge used to populate the metastable levels is indicated by the dashed line

the three beams in the interaction region. The phase conjugated beam, after being appropriately deflected, was detected by a photodiode (PD 1) and was recorded with the assistance of a boxcar integrator (BC) connected to an analogue recorder (X-Y).

The HPO used for the production of the Ca vapour was equipped with a temperature stabilisation system, capable of producing temperatures up to $\sim 1000^\circ\text{C}$ and maintaining them constant to within 0.5%. For the reduction of the strong absorption by the Ca vapour at the resonance frequency, the HPO was designed in such a way that the length of the vapour column was not much longer than the beam overlap region, estimated to be on the order of 2–3 cm. When the OPC effect is observed via highly excited states $4p^2\ ^3P_{0,1,2}$ (see Fig. 1) the experimental scheme could become quite complicated since additional laser beams are required for the excitation of the atoms from the ground state. In order to avoid this complication, appropriate electrodes had been fitted in the HPO set-up to generate an electric discharge that collisionally excited the Ca atoms to their metastable states. From these metastable states a realisation of the DFWM technique similar to the one described above was used. The N_2 -pumped dye laser system (the stilbene 420 dye (Exciton) was used) was tuned on and around the wavelengths corresponding to the six possible transitions from the metastable states $4s4p\ ^3P_{0,1,2}$ to the manifold of the $4p^2\ ^3P_{0,1,2}$ states. Additionally, this set-up offers the possibility for the simultaneous recording of an optogalvanic signal, that can be used as a reference for the measurement of the conjugate wave characteristics. The wavelength of the laser beams is periodically checked by a λ -meter.

2 Theoretical model

In order to take into account the effect of absorption we assume exponential attenuation of the two pump beams as they

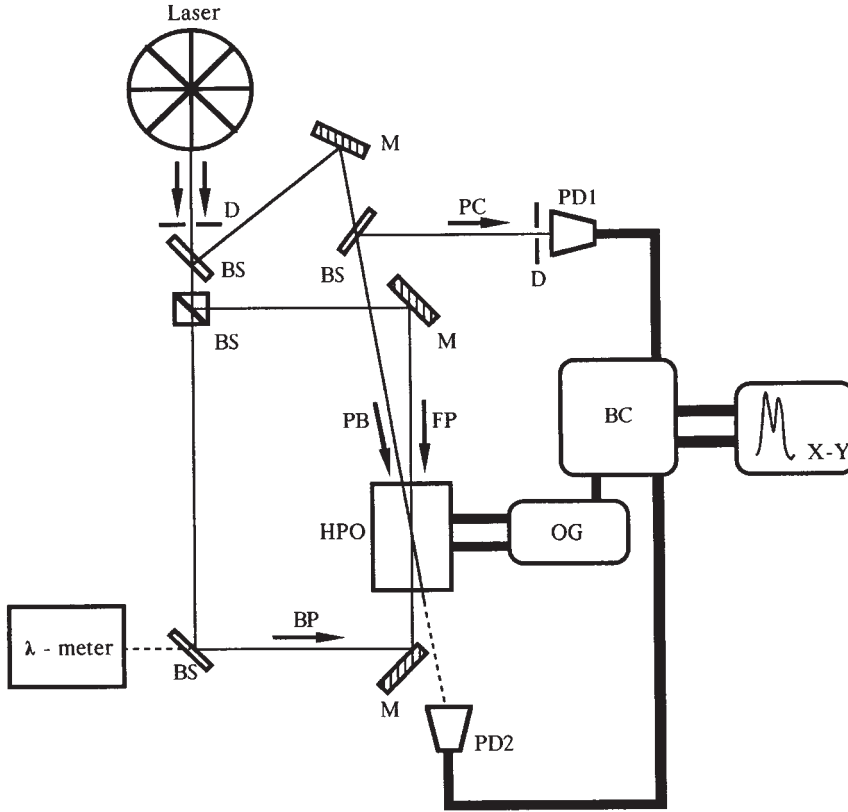


Fig. 2. Experimental set-up. BS: beam splitter, M: mirror, PD1 & PD2: photodiodes, HPO: Heat-Pipe Oven, OG: optogalvanic device, BC: boxcar averager, X-Y: chart recorder, BP: backward pump beam, FP: forward pump beam, PB: probe beam, PC: phase conjugated beam

propagate through the medium along the z -axis. The attenuation coefficient, α , will in general have a spatial dependence, whose exact form will be determined by, among other factors, the density distribution of Ca atoms in the vapour column. To simplify the model we introduce [18] a z -averaged attenuation coefficient, $\bar{\alpha}$, and write for the spatial evolution of the forward and backward pump intensities the expressions

$$I_f(z) = I_{f0} \exp(-2\bar{\alpha}z), \quad (1)$$

$$I_b(z) = I_{b0} \exp[-2\bar{\alpha}(L-z)] \quad (2)$$

where I_{f0} and I_{b0} are, respectively, the forward and backward pump intensities before attenuation, and L is the interaction length. The average attenuation coefficient is determined through the equation

$$\bar{\alpha} = \alpha_0 \frac{1}{1+\delta^2} \frac{1}{L} \int_0^L \frac{1 + \frac{I_f+I_b}{I_{\text{sat}}}}{\left[\left(1 + \frac{I_f+I_b}{I_{\text{sat}}}\right)^2 - 4 \frac{I_f I_b}{I_{\text{sat}}^2} \right]^{\frac{3}{2}}} dz \quad (3)$$

where α_0 is the unperturbed line-center absorption coefficient [19], δ is the normalised detuning from resonance, $\delta = (\omega - \omega_{12})/\gamma_2$, where γ_2 is the coherence decay rate, and I_{sat} is the frequency-dependent saturation intensity [19]. Then the intensity of the phase conjugated beam at the end of the interaction region, $I_s(L)$, can be calculated. Equivalently, one obtains the reflectivity, $R = I_s(L)/I_{p0}$, where I_{p0} is the probe beam intensity before attenuation. Without going into the details of the derivation (see [18]), we quote the final result

$$R = \frac{|\bar{\beta}|^2}{4|\bar{\alpha}|^2} [1 - \exp(-2\bar{\alpha}L)]^2 \quad (4)$$

where the z -averaged non-linear coupling coefficient, $\bar{\beta}$, is given by the expression

$$\bar{\beta} = \alpha_0 \frac{i + \delta}{1 + \delta^2} \frac{1}{L} \int_0^L \frac{2 \frac{(I_f I_b)^{\frac{1}{2}}}{I_{\text{sat}}}}{\left[\left(1 + \frac{I_f+I_b}{I_{\text{sat}}}\right)^2 - 4 \frac{I_f I_b}{I_{\text{sat}}^2} \right]^{\frac{3}{2}}} dz \quad (5)$$

evaluated for the value of $\bar{\alpha}$ obtained by solving equation (3).

3 Results and discussion

In Fig. 3 the dependence of the maximum of the PC signal on the total input laser intensity, I_0 , is shown. The relative intensities of the interacting beams were adjusted so as to have $I_{f0} = I_{b0} = 5I_{p0}$. The maximum input intensity employed in the experiment was $\sim 20 \text{ kW/cm}^2$. The ground-state Ca concentration was kept very low, roughly $3 \times 10^{11} \text{ cm}^{-3}$, in order to minimize the effects of absorption. The buffer gas pressure was kept to 0.66 kPa. For low input intensities ($\sim 0.5 \text{ kW/cm}^2$) the signal exhibits a power law dependence with exponent ~ 2.4 , roughly corresponding to a cubic intensity dependence [7]. For higher input intensities the dependence clearly deviates from the cubic power law and the onset of saturation is evident in the upper end of the intensity range employed in our experiments. The results of our model calculations reproduce this behaviour. The experimentally determined intensities had to be scaled down by a factor 0.16 in order to obtain the fit between theory and experiment. This takes into account the fact that from the spectrally distributed input laser intensity only the fraction lying within the atomic linewidth contributes to the effect [18]. All other parameters employed in the calculations were as determined experimentally.

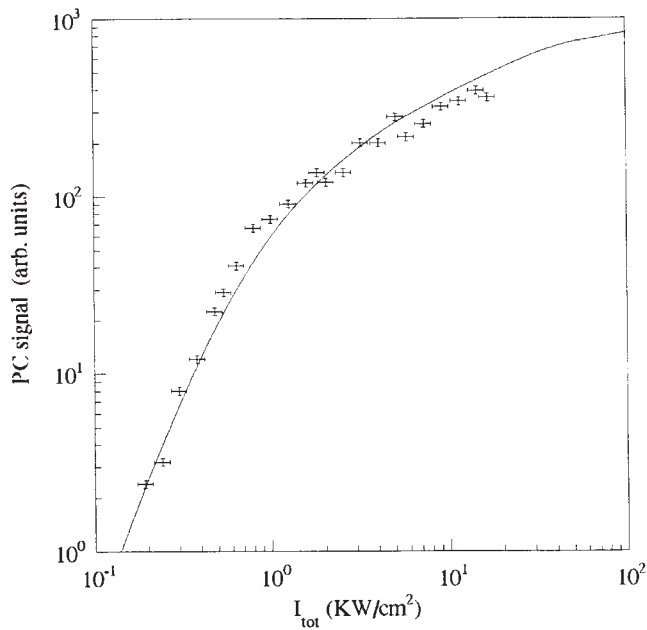


Fig. 3. PC signal (maximum) vs. total input intensity. The symbols correspond to the experimental points and their associated error bars. The continuous line is the result of theoretical calculations, for which the parameters used were: $N_{\text{Ca}} = 3 \times 10^{11} \text{ cm}^{-3}$, $P_{\text{He}} = 0.66 \text{ kPa}$

For the sake of completeness the dependence of the PC signal on the probe beam intensity was studied under the same experimental conditions as for the results in Fig. 3. The experimental results are shown in Fig. 4 along with a line of slope 0.9, representing the best linear fit to the data. This is in fair agreement with the expected linear intensity dependence [7], when a weak probe is employed in DFWM in a non-absorbing medium. These conditions are nearly met in our experiment since the highest intensity used was $I_{\text{PB}} \sim 4 \text{ kW/cm}^2$ and the Ca concentration was sufficiently low to consider absorption negligible.

Figure 5 shows typical spectra of the PC beam intensity as a function of laser frequency, in the vicinity of the $4s4p^1P_1$ state of Ca, for three different values of the Ca concentration. Tabulated values of the Ca vapour pressure were used [20] for the evaluation of the Ca concentration. The temperature was measured at the center of the HPO with an appropriately attached thermocouple. The spectra were taken at a constant buffer gas pressure of 0.93 kPa. We used He as a buffer gas. The intensities of the input beams before entering the HPO were measured to be $I_{f0} = I_{b0} \sim 25 \text{ kW/cm}^2$ and $I_{p0} \sim 5 \text{ kW/cm}^2$. As the Ca concentration was increased, an increase of the phase conjugated signal was observed accompanied by the appearance of a dip at line center, giving rise to a symmetrical double peak structure. The slight asymmetry in the peak heights is probably due to propagation effects other than the linear absorption. Further increasing the Ca number density to values higher than 10^{16} cm^{-3} resulted in a lower peak intensity for the phase conjugated beam but also in a wider dip that has virtually eliminated any generated intensity within a wide frequency range (4 cm^{-1}) around the line center and has shifted further apart the two peaks of the generated signal. This is clearly due to the effect of saturated absorption at line center. This conclusion is further supported by the reproduction of the experimentally observed features

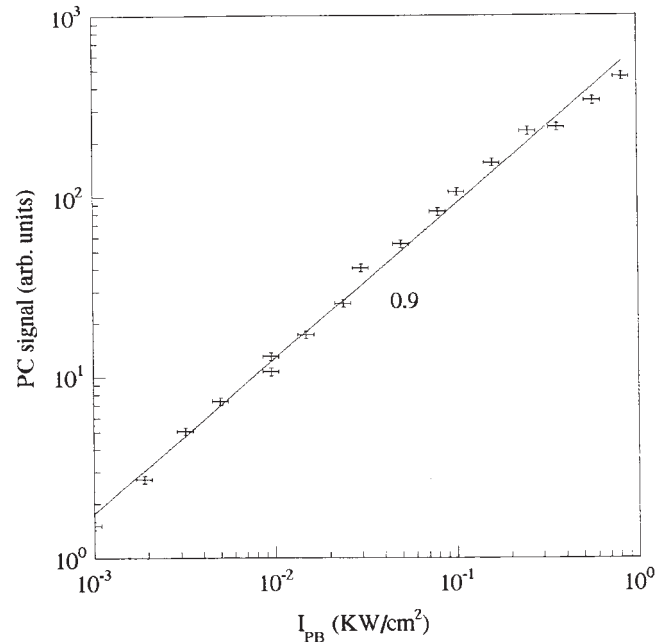


Fig. 4. PC signal (spectrally integrated) vs. probe beam intensity. The continuous line is the best linear fit to the data. The slope is 0.9, as shown on the figure

by our model calculations that take into account explicitly, albeit in an average way, the effect of absorption. All three theoretical spectra shown in Fig. 5 have been obtained using the experimentally measured values for the Ca number density and the buffer gas pressure. The only exception is the Ca number density for the spectrum in Fig. 5a that was taken to be $1.13 \times 10^{13} \text{ cm}^{-3}$ or 45% lower compared to the experimentally determined value. It is conceivable that at relatively low Ca concentrations, where absorption is rather weak, an average attenuation coefficient might overestimate the effect of absorption on the spectra. The buffer gas pressure, determining the dephasing rate γ_2 through an appropriate cross section for dephasing collisions (see below), had only minor influence on the details of the spectra when varied between 0.13 kPa and 1.3 kPa, i.e. in the pressure range around the actual value used in the experiment. In all three cases the theoretical spectra were adjusted to the maximum of the experimental data through an appropriate scaling factor. Our main concern at this point was the reliable reproduction of the spectral features. To this end we have also convoluted the theoretical spectra with a normalised Gaussian of 0.5 cm^{-1} width to take into account the finite resolution because of the specific laser lineshape.

It is also interesting, however, to know the dependence of the PC signal on the number density in a wide range of values for this parameter. In Fig. 6 the experimental results for the maximum PC signal vs. the Ca number density are shown, together with a curve obtained with our theoretical model. The agreement between the two is satisfactory in the rising part of the curve, corresponding to low and medium number densities. The slope of the log-log plot in this range is ~ 1.8 , quite close to the result expected on the basis of theoretical predictions for a quadratic concentration dependence of the PC signal in an optically thin medium interacting with low intensity beams [2]. Since the intensities employed in our

experiment were above the saturation intensity and the onset of significant absorption is evident for Ca densities on the order of $4 \times 10^{14} \text{ cm}^{-3}$, an exact quadratic dependence is not to be expected. The PC signal reaches a maximum for Ca number densities between $5 \times 10^{14} \text{ cm}^{-3}$ and 10^{15} cm^{-3} , while for still higher concentrations it gradually decreases as the absorption dominates the generation of the phase conjugated beam. This behaviour is qualitatively reproduced by our theoretical model, that clearly overestimates the degree of absorption, probably because of the average way in which it is taken into account.

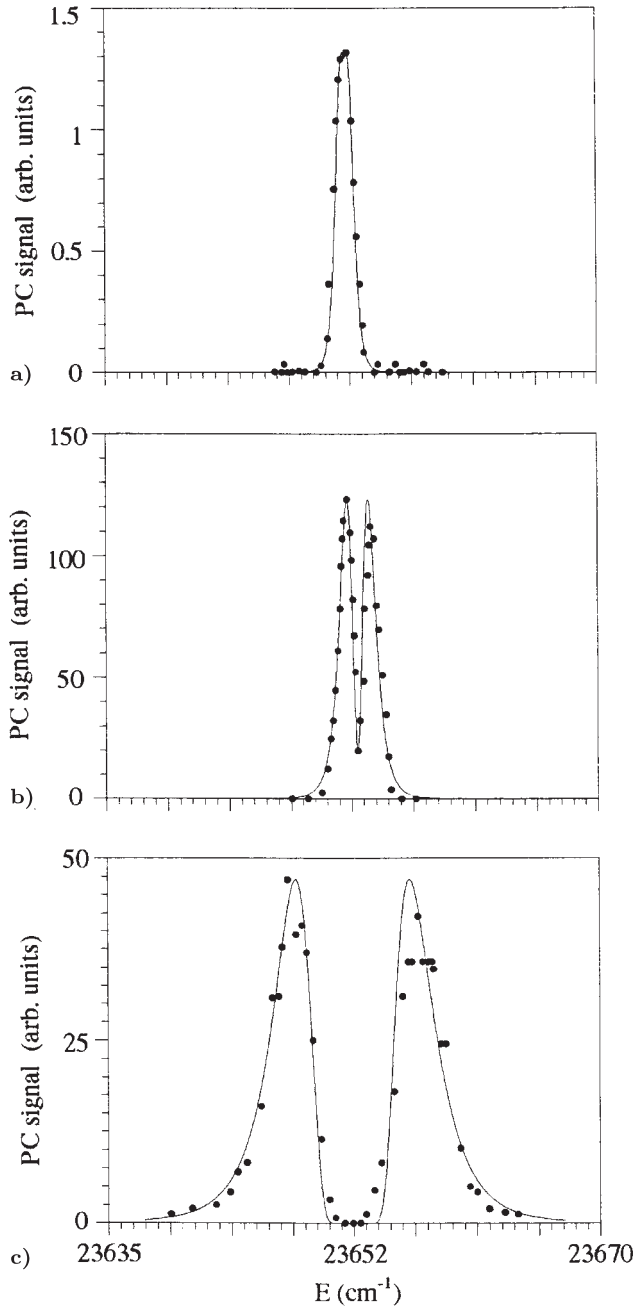


Fig. 5a–c. PC signal vs. laser frequency for three different Ca concentrations (a) $N_{\text{Ca}} = 2.5 \times 10^{13} \text{ cm}^{-3}$, (b) $N_{\text{Ca}} = 4.6 \times 10^{14} \text{ cm}^{-3}$, (c) $N_{\text{Ca}} = 1.37 \times 10^{16} \text{ cm}^{-3}$. The intensities of the input beams were $I_{f0} = I_{b0} \sim 25 \text{ kW/cm}^2$. The dots are experimental points, the continuous line is the result of theoretical calculations

A similar behavior has been observed when a cell of iodine vapor was used in a DFWM experiment [18]. However, signal saturation sets in at number densities almost two orders of magnitude higher than those encountered in our Ca results, despite the fact that iodine is considered to be a strongly absorbing molecular gas.

In the environment of the HPO the presence of the buffer gas is important (it is He in our case) for creating, maintaining and controlling a Ca vapour column. Its influence on the generation of the PC signal in Ca is mainly due to dephasing collisions between buffer gas atoms and Ca atoms in the excited state. Collisional quenching has also been known to strongly affect the PC signal especially in molecular media [21] but is negligible under our conditions. We, therefore, introduce for the dephasing rate the expression

$$\gamma_2 = \frac{\gamma_{\text{nat}}}{2} + \gamma_c^{(0)} p \quad (6)$$

where γ_{nat} is the spontaneous decay rate [22] of the $4s4p \ ^1P_1$ state, $\gamma_c^{(0)}$ is the appropriate collisional rate [23] at line-center, and p the pressure. We have used the value $\gamma_c^{(0)} = 3.13 \times 10^8 \text{ s}^{-1} \text{ kPa}^{-1}$ in all theoretical calculations. In Fig. 7 spectra of the PC signal at various buffer gas pressures are shown. The chosen values of buffer gas pressure cover the entire range investigated at the experiment. The Ca number density was $\sim 3 \times 10^{14} \text{ cm}^{-3}$; at this density absorption is significant but not saturated. The measured pump intensities were $I_{f0} \sim 20 \text{ kW/cm}^2$ and $I_{b0} \sim 30 \text{ kW/cm}^2$, while $I_{p0} \sim 10 \text{ kW/cm}^2$. The effect of absorption at line center is again evident in the symmetrical double-peaked structure of the spectra. However, unlike the spectra in Fig. 5, the signal maxima are detuned by not more than 25 GHz from resonance and the detuning is nearly pressure independent within the en-

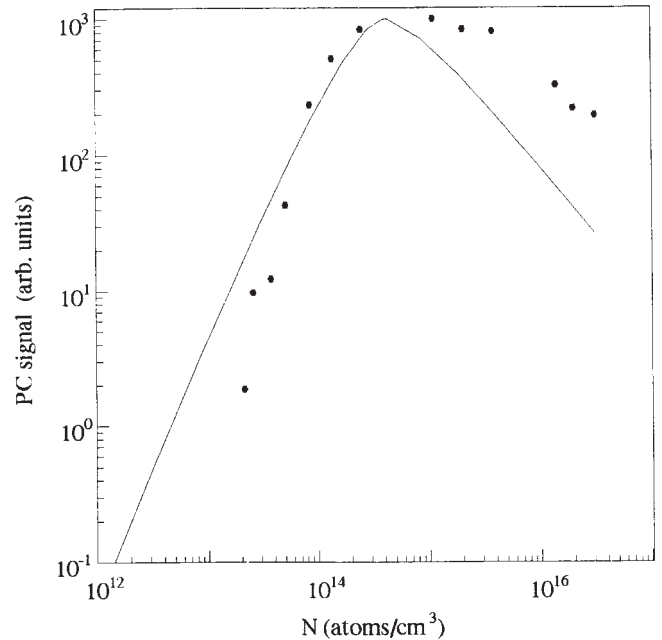


Fig. 6. PC signal (maximum) vs. Ca concentration. The dots are experimental points, the continuous line is the theoretical result. The input beam intensities were $I_{f0} = I_{b0} \sim 25 \text{ kW/cm}^2$. For the calculations the length of the medium was taken to be $L = 5 \text{ cm}$ and the buffer gas pressure $P_{\text{He}} = 0.66 \text{ kPa}$

tire range of buffer gas pressures investigated (0.3–93.3 kPa). This behaviour is reproduced by our theoretical model, although the Ca vapour densities employed in the calculations were lower compared to the experimentally determined ones, especially for the high-pressure spectra. Theoretical fits of equally good quality could be obtained by decreasing the value of $\gamma_c^{(0)}$ by the same factor (see the caption of Fig. 7). This

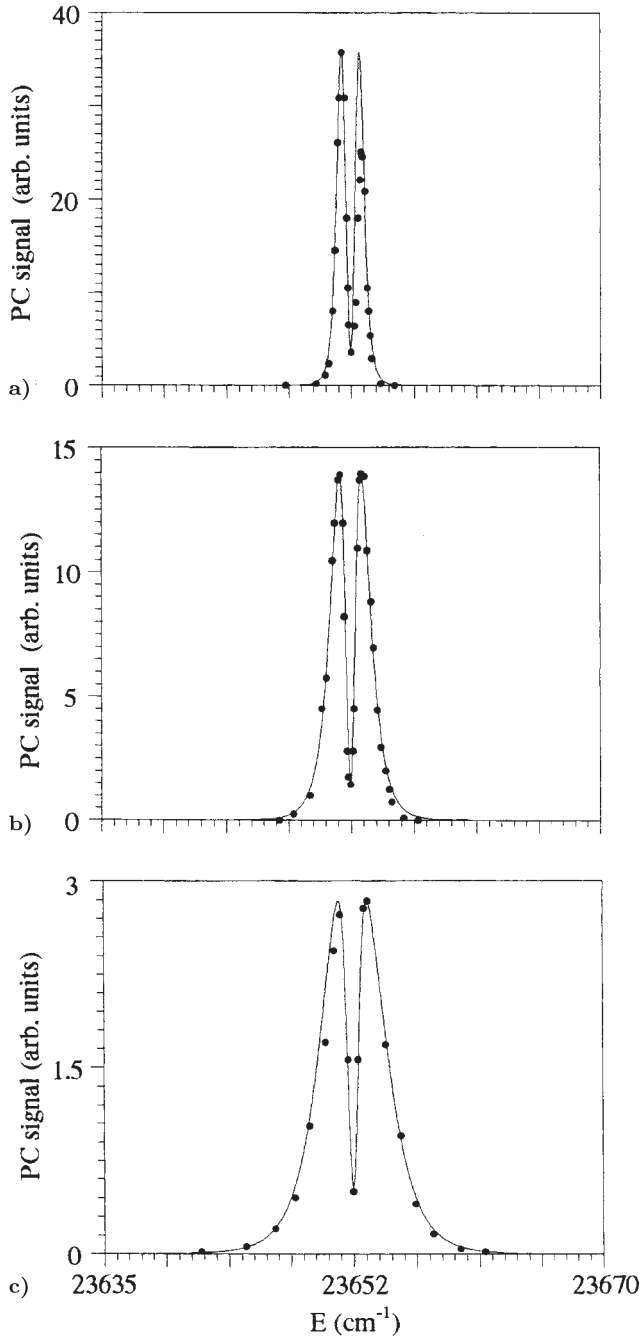


Fig. 7a–c. PC signal vs. frequency for three different buffer gas pressures: (a) $P_{\text{He}} = 1.33$ kPa, (b) $P_{\text{He}} = 26.66$ kPa, (c) $P_{\text{He}} = 93.3$ kPa. The dots are experimental points, the continuous line is the theoretical result. For the theoretical calculations the Ca vapour density was reduced by 0.5, 0.05 and 0.04 compared to the experimental values for cases (a), (b) and (c) respectively. The medium length was taken to be $L = 5$ cm in all cases

indicates that the buffer gas and Ca vapour were not mixed homogeneously for the whole interaction length, with a possible exception for the highest pressures. In addition, the interaction length was assumed constant while it is well known that in HPO devices a low buffer gas pressure leads to an increased vapour column and larger spatial inhomogeneities. Thus the lowering of the vapour density in the calculation correctly reflects this behaviour. As in Fig. 5 earlier, the theoretical spectra in Fig. 7 were fitted by a scaling factor to the maximum of the experimental data and were convoluted with a Gaussian of 0.5 cm^{-1} width.

The global dependence of the maximum of the PC signal on the buffer gas pressure, for given Ca concentration and pump beam intensities, is shown in Fig. 8. The experimental data show a steep decrease of the PC signal as the buffer gas pressure is increased up to a value of 53.3 kPa. For higher pressures the decrease is considerably slower and the signal can easily be detected, although less intense, for pressures up to 93.3 kPa. This behaviour is analogous to the one observed in Ba [12] a system quite similar to Ca as far as the electronic structure is concerned. The theoretical curve reproduces the observed behaviour. The agreement is excellent for buffer gas pressures above 40 kPa. The model fails to predict the signal behaviour at pressures below 6.5 kPa. In this range, the theoretical value shows a steep increase that is qualitatively different from the experimental observation. For low pressures the medium broadening is no longer dominated by collisions [21] and other mechanisms, e.g. Doppler broadening, may dominate. However, these mechanisms are not taken into account in our modelling. Also not taken into account is the effect of pump depletion [10]. All of the above in addition to possible inhomogeneities in the vapour density necessitate a far more detailed modelling than the one attempted here [24].

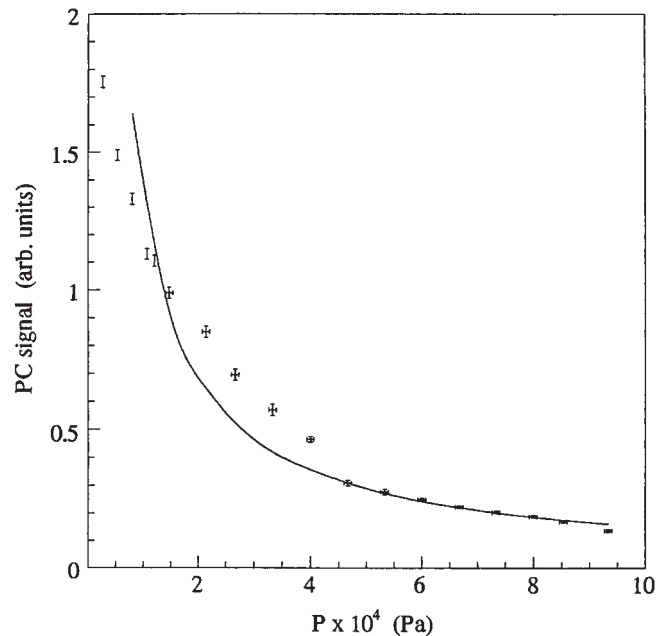


Fig. 8. PC signal (maximum) vs. buffer gas pressure. The symbols correspond to the experimental points and their associated error bars. The input beam intensities were $I_{f0} \sim 20 \text{ kW/cm}^2$, $I_{b0} \sim 30 \text{ kW/cm}^2$, and $I_{p0} \sim 10 \text{ kW/cm}^2$. The continuous line is the result of theoretical calculations, for which $N_{\text{Ca}} = 3 \times 10^{14} \text{ cm}^{-3}$

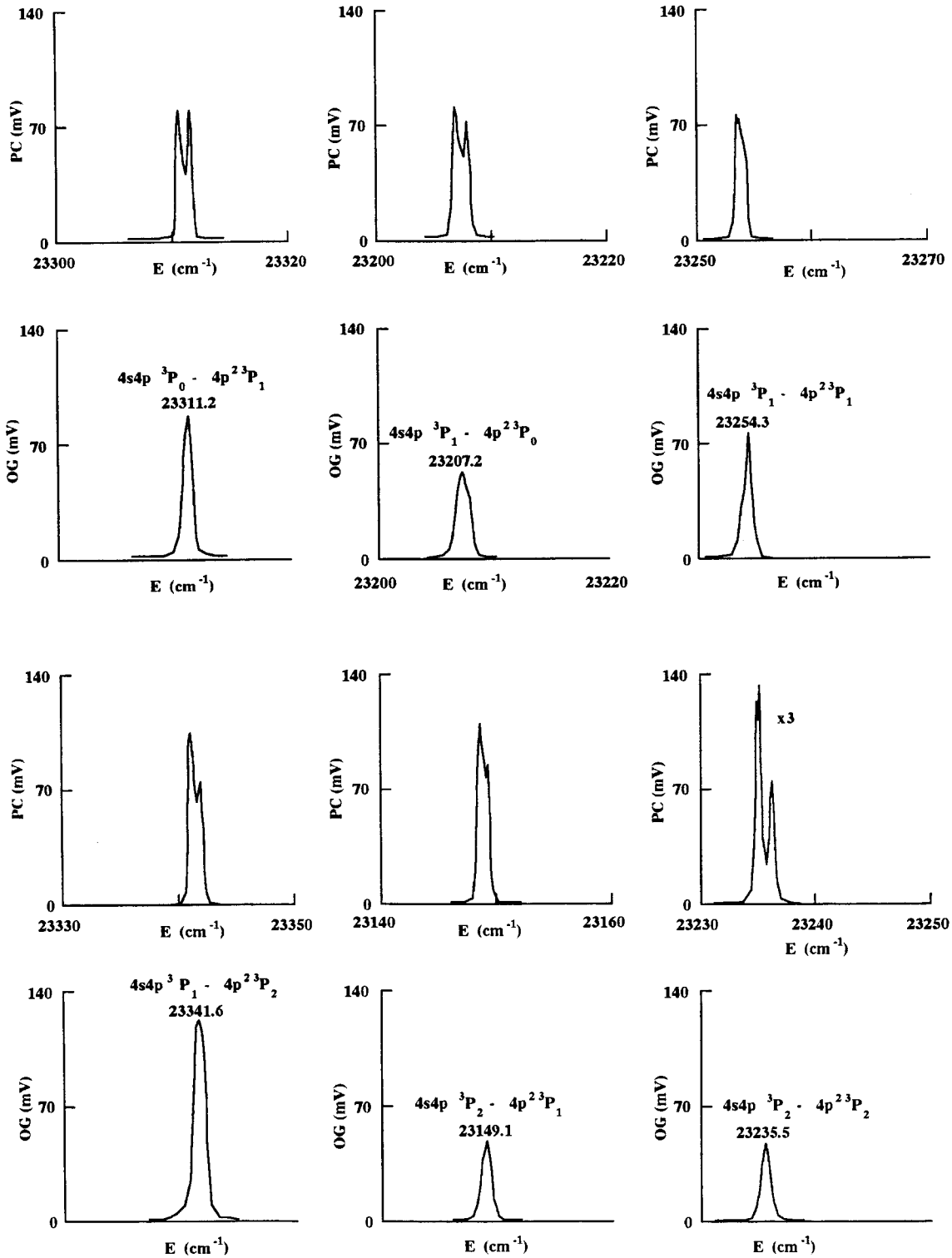


Fig. 9. PC signal vs. frequency and optogalvanic signal vs. frequency for all six allowed transitions $4s4p\ ^3P_J \rightarrow 4p^2\ ^3P_J$, $J = 0, 1, 2$. The optogalvanic signal peak characterizes the transition frequency, whose value is also shown. In the plot corresponding to the $4s4p\ ^3P_2 \rightarrow 4p^2\ ^3P_2$ transition the PC signal has been scaled down by a factor of 3 to fit in the same vertical scale as the rest

The reflectivity R , which measures the efficiency of the phenomenon, was measured under various experimental conditions. The highest value measured was $\sim 46\%$ for $I_{f0} = I_{b0} = 5I_{p0}$, $N_{Ca} = 4 \times 10^{15} \text{ cm}^{-3}$ and $P_{He} = 1.3 \text{ kPa}$. This reflectivity, although higher than the corresponding one in Ba [12], is not considered to be particularly large. It could be

improved, if that was necessary, by changing a number of design parameters in our set-up. One such parameter is the actual length of the vapour column of the active medium, which if further reduced to match exactly the length of the beam overlap region would lead to appreciable increase of the reflectivity by reducing the absorption of the generated beam.

The final step in our study was the investigation of OPC via the highly excited bound states $4p^2\ ^3P_{0,1,2}$ of Ca. These states were laser excited from the metastable $4s4p\ ^3P_{0,1,2}$ ones, efficiently populated by collisional excitation in the electric discharge environment created in the HPO. In Fig. 9 the PC spectra of the six allowed transitions, $4s4p\ ^3P_{0,1,2} \rightarrow 4p^2\ ^3P_{0,1,2}$, together with the simultaneously recorded corresponding optogalvanic spectra, are shown. The experimental conditions during the recording of these spectra were $I_{\text{tot}} \sim 50 \text{ kW/cm}^2$, $I_{f0} = I_{b0} = 5I_{p0}$, $N_{\text{Ca}} = 3 \times 10^{15} \text{ cm}^{-3}$ and $P_{\text{He}} = 0.66 \text{ kPa}$. A simple theoretical model [19] predicts that the spectrally integrated PC signal under strong pumping scales according to the relation

$$I_{\text{PC}} \sim \mu_{12}^3 \tau_2^{-\frac{1}{2}} \quad (7)$$

where μ_{12} is the dipole moment for the transition from the $4s4p\ ^3P_J$ manifold to the $4p^2\ ^3P_J$ one and τ_2 the spontaneous decay lifetime of the final state. Using the atomic parameters for the specific states and transitions [22] we find that the dependence predicted by theory is in fair agreement with the experimental data, although our experimental conditions do not exactly correspond to the assumptions of the model. The reflectivity for these transitions was measured under various experimental conditions. Since the population of the metastable Ca states, the initial states of the DFWM scheme, strongly depends on the electric discharge parameters, so does the PC signal. For the highest attainable discharge current in our set-up the highest reflectivity measured was $\sim 46\%$ for the transition $4s4p\ ^3P_2 \rightarrow 4p^2\ ^3P_2$. This result is qualitatively consistent with the cubic dependence on the μ_{12} value shown in (7) given the fact that for the above mentioned transition the μ_{12} value is the highest among the allowed six. This result is encouraging for extending the study of the phenomenon in the energy range where AIS can be found. However, a number of non-trivial difficulties have to be resolved before one could proceed in such an experiment and we comment on these in the following section.

4 Conclusions

The OPC phenomenon was studied in Ca vapour via the bound states $4s4p\ ^1P_1$ and $4p^2\ ^3P_{0,1,2}$, using the DFWM technique. In both cases by optimizing the experimental conditions the efficiency of the phenomenon reached $\sim 46\%$, providing additional evidence that the alkaline earths are suitable as non-linear media. The dependence of the signal as a function of Ca concentration, buffer gas pressure and total pump intensity, was recorded. Strong absorption affected the experimental results and a theoretical model taking absorption into account in an average way was employed in order to interpret the results. The agreement between theory and experiment was satisfactory for most of the data. The few discrepancies were clearly attributable to the lack of sufficient detail in our model.

Our results suggest that in a rather complicated environment like the one found in a HPO, the DFWM technique can lead to a strong PC signal reflecting the behaviour of a non-linear material in such an environment. The results can be understood almost quantitatively by a rather simple theoret-

ical model. However, a number of serious limitations exist, strong absorption being one of them, that restrict the applicability of the technique in a reliable way outside certain ranges for the externally controlled parameters (concentration, pump intensity, buffer gas pressure). Ingenious experimental arrangements would have to be made to overcome these limitations. In addition, our results have shown promise for extending the study of OPC by DFWM in the vicinity of AIS. The short lifetimes of AIS (normally a few ps or even sub-ps) necessitate the use of comparably short excitation pulses. Moreover, large photon energies (in the VUV) are needed if one attempts to reach AIS from the ground atomic state by one-photon processes. Recent progress has led to the development of a new source of high-energy (VUV to XUV), short duration (sub-ps), coherent, partly tunable photons that could be ideal for such applications. We refer to the high-order harmonics generated from a gas medium (usually a rare gas) when irradiated by strong, short laser pulses in the optical or infrared frequency range [25]. Alternatively, one might use coherent or incoherent processes to excite the atomic system to a bound long-lived state (e.g. a metastable one like the $4s4p\ ^3P_J$ of Ca) and then apply optical photons to reach selected AIS by resonant DFWM. In both potential configurations the experimental complexity is evident; also evident is the importance of the successful demonstration of the OPC effect by resonant DFWM via AIS, particularly when XUV photons are involved. Towards this goal we are currently working.

References

1. R.A. Fisher: *Optical Phase Conjugation*, (Academic Press, 1983)
2. D.C. Hanna, M.A. Yuratich, D. Cotter: *Non-linear optics of free atoms and molecules* (Springer, Berlin, Heidelberg 1979)
3. J. Gumbel, W. Kiefer: Chem. Phys. Lett. **189**, 231 (1992)
4. R.L. Farrow, D.J. Rakestraw: Science **257**, 1894 (1992)
5. (a) C. Halvorson et al.: Science **265**, 1215 (1994); (b) B. Ai et al.: Appl. Phys. Lett. **64**, 951 (1994);
6. C.R. Vidal: In *Topics in Applied Physics*, vol. 59, chap. 3 (Springer, Berlin, Heidelberg 1986)
7. R.L. Abrams, C.R. Lind: Opt. Lett. **2**, 94 (1978); *ibid.* **3**, 205 (1978)
8. (a) D. Bloch, M. Ducloy: J. Opt. Soc. Am. **73**, 635 (1983); (b) G. Grynberg et al.: Opt. Comm. **50**, 261 (1984); (c) M. Pinarid et al.: Opt. Comm. **51**, 281 (1984)
9. S. Singh, G.S. Agarwal: J. Opt. Soc. Am. B **5**, 2515 (1988)
10. W.P. Brown: J. Opt. Soc. Am. **73**, 629 (1983)
11. A.L. Gaeta et al.: IEEE J. Quant. Elec. **QE-25**, 373 (1989)
12. T. Mikropoulos et al.: Opt. Lett. **15**, 1270 (1990)
13. Z. Wu, W.G. Ton: Spectrochim. Acta **3**, 449 (1992)
14. M. Aymar, C. Greene, E. Luc-Koenig: Rev. Mod. Phys. **68**, 1015 (1996)
15. O. Faucher et al.: Phys. Rev. A **50**, 641 (1994)
16. P. Ljungberg, O. Axner: Appl. Phys. B **59**, 53 (1994)
17. (a) P. Ewart, S.V. O'Leary: Opt. Lett. **711**, 279 (1986); (b) T. Dreier, D.J. Rakestraw: Opt. Lett. **15**, 72 (1990); (c) D.J. Rakestraw et al.: Opt. Lett. **715**, 709 (1990); (d) B.A. Mann et al.: Appl. Phys. B **54**, 271 (1992)
18. J. Gumbel, W. Kiefer: J. Opt. Soc. Am. B **9**, 2206 (1992)
19. R.L. Farrow, D.J. Rakestraw, T. Dreier: J. Opt. Soc. Am. B **9**, 1770 (1992)
20. A.N. Nesmeyanov: *The Vapour Pressure of the Chemical Elements*, (Elsevier, Amsterdam, New York 1963)
21. P. Barker et al.: Appl. Optics **34**, 3281 (1995)
22. W.L. Wiese, G.A. Martin: *Wavelengths and Transition Probabilities for Atoms and Atomic Ions* NSRDS-NBS 68, US Gov. Printing Office, Washington DC (1980)
23. N. Allard et al.: Rev. Mod. Phys. **54**, 1103 (1982)
24. R.P. Lucht, R.L. Farrow, D.J. Rakestraw: J. Opt. Soc. Am. B **10**, 1508 (1993)
25. Ph. Balcou et al.: Z. Phys. D **34**, 107 (1995)